


Cite this: *RSC Adv.*, 2024, 14, 37752

# A review on the multifaceted effects of $\delta$ -MnO<sub>2</sub> on heavy metals, organic matter, and other soil components

Haoran Hu,<sup>a</sup> Xiang Li,<sup>b</sup> Xinyu Gao,<sup>a</sup> Lei Wang,<sup>a</sup> Bo Li,<sup>a</sup> Fandong Zhan,<sup>a</sup> Yongmei He,<sup>a</sup> Li Qin<sup>\*a</sup> and Xinran Liang<sup>\*a</sup>

Manganese oxide minerals are prevalent in soils and play a pivotal role in the immobilization of heavy metals and the transformation of materials. Characterized by their low point of zero charge and numerous active adsorption sites, manganese oxides effectively accumulate heavy metals such as lead (Pb) and cadmium (Cd) from contaminated environments. Different manganese oxides, mediated by Mn(II), vary in their capacity to enrich heavy metals. Their distinctive nanostructures can be harnessed to create composite materials that boast enhanced adsorption properties and environmental sustainability. As a highly reactive element in soil, manganese engages in multiple reactions with soil organic components and inorganic ions through processes like oxidation-reduction. This activity aids in the elimination of organic pollutants and facilitates carbon sequestration through various mechanisms. This article explores the metal enrichment capabilities of manganese oxides and their influence on soil physicochemical properties, enhancing our understanding of how these oxides adsorb metallic elements and interact with soil components. Such knowledge is crucial for advancing heavy metal remediation strategies and comprehending the biogeochemical processes within soil environments.

Received 19th August 2024  
Accepted 8th November 2024

DOI: 10.1039/d4ra06005a

rsc.li/rsc-advances

## 1 Introduction

As soil metal contamination increasingly threatens human health and well-being, there is a growing focus on mitigating the pollution of metal elements. Soils and sediments contain a variety of minerals, among which iron and manganese oxides, along with their hydroxides, represent a significant component. Despite constituting only a fraction of the total solid phase in soils or sediments, these oxides and hydroxides play a crucial role due to their high adsorption capacities, they significantly influence the mobility and bioavailability of trace metal pollutants.<sup>1</sup> Manganese oxides, in particular, often form surface coatings on soil particles and nodules. Although present in relatively low concentrations, manganese oxides have a higher redox potential and stronger adsorption affinity compared to iron oxides, enhancing their capacity to accumulate metal elements.<sup>2</sup> Table 1 showcases the adsorption capacities of these manganese oxide minerals for heavy

metals, emphasizing their importance in soil remediation efforts.<sup>3–7</sup>

Manganese oxides, capable of existing in multiple valence states (II, III, IV), form a variety of minerals such as manganite, cryptomelane, and birnessite.<sup>3</sup> These minerals are pivotal in enriching soil with metal ions like Pb, Cd, and Co through mechanisms like adsorption and isomorphic substitution.<sup>8,9</sup> They also play a role in the migration of various metals (Pb, Cu, Ni, Cr) and metalloids (As) within the soil. However, the role of manganese oxides extends beyond mere enrichment of metal elements. The interaction of manganese oxides with complex soil components—organic matter, oxyanions, and cations—and environmental factors like pH and Eh leads to structural and morphological changes.<sup>10,11</sup> These transformations result in various crystalline forms of manganese oxide minerals, influencing the migration, bioavailability, and toxicity of metals in soils.<sup>13–15</sup>

Moreover, manganese's role as a bio-oxidative metal is vital in the carbon cycle of terrestrial ecosystems, it facilitates the deposition of organic substances within mineral-rich soils and sediments, thereby influencing carbon migration and transformation.<sup>16,17</sup> The multifaceted interactions of manganese oxides with soil components are critical in stabilizing soil ecosystems. This has led to significant research interest across various disciplines, highlighting the importance of manganese oxides in environmental science and soil remediation.

<sup>a</sup>College of Resources and Environment, Yunnan Agricultural University, Kunming 650201, China. E-mail: hhr2283367202@163.com; 1841336079@qq.com; wanglei.ko@foxmail.com; ecolibo@126.com; zfd97@ynau.edu.cn; eyongmei06@126.com; qinli2975@ynau.edu.cn; lxr8900@live.com

<sup>b</sup>Flower Research Institute of Yunnan Academy of Agricultural Sciences, Yunnan Provincial Key Laboratory of Flower Breeding, National Engineering Research Center for Ornamental Horticulture, Yunnan Seed Laboratory, Kunming, 650205, China. E-mail: lixiang@yaas.org.cn



Table 1 Adsorption of heavy metal elements by different manganese oxide minerals<sup>3,4</sup>

Minerals	Mineral structure	Adsorption of heavy metal elements (mmol kg <sup>-1</sup> )				
		Pb	Co	Cu	Cd	Zn
Birnessite	Mn <sup>4+</sup> layered structure	1832	1084	1268	1042	1207
Cryptomelane	Mn <sup>4+</sup> tunnel structure	292.8	75.5	132.5	88.8	87.1
Todorokite	Mn <sup>4+</sup> tunnel structure	284.3	117.3	191.4	85.1	67.3
Hausmannite	Low-valence manganese	105.3	44.4	189	3.3	43.1

## 2. Enrichment of metal elements by manganese oxides

Long-term heavy metal pollution poses significant risks to arable soil and human health, with cadmium (Cd) and lead (Pb) being common contaminants that infiltrate soil and water bodies through anthropogenic activities.<sup>18,19</sup> Manganese oxides are particularly noted for their negatively charged surfaces and distinctive nanostructures, making them valuable for adsorbing, immobilizing, and transferring heavy metals. Manganese oxides can also be combined with other adsorbents and reducing agents to enhance remediation efforts.

$\delta$ -MnO<sub>2</sub>, a primary form of manganese oxide, can evolve into other secondary manganese oxide minerals.<sup>3</sup> This transformation is influenced by its interaction with heavy metal ions, which is closely linked to its crystal structure. The structure of  $\delta$ -MnO<sub>2</sub> consists of disordered layers of [MnO<sub>6</sub>] octahedra and water molecules, within the [MnO<sub>6</sub>] octahedral layer, vacancies caused by low-valence manganese substitution or manganese deficiency, alongside [Mn(III)O<sub>6</sub>] octahedra arranged in a shared-apex configuration, contribute to the negative charge of  $\delta$ -MnO<sub>2</sub>.<sup>20–22</sup> This negative charge is crucial for the electrostatic adsorption of cationic pollutants.<sup>23</sup>

Birnessite, a type of  $\delta$ -MnO<sub>2</sub> with a low point of zero charge (PZC < 3), is effective in removing metal cations across a broad pH range through adsorption and co-precipitation.<sup>24,25</sup> Fig. 1 illustrates the mechanisms of metal ion enrichment by manganese oxides, where adsorption typically involves electrostatic attraction at the solid/liquid interface, and co-precipitation includes both this interfacial binding and the formation of surface precipitates from metal oxides.<sup>26</sup> Manganese oxides are integral to the biogeochemical cycles of trace metals and metalloids, significantly influencing the bioavailability and mobility of these elements in the environment.<sup>27–29</sup>

### 2.1 Enrichment of Cd by manganese oxides

Cd(II) is commonly found in soils as hydroxides or carbonate precipitates. Manganese oxides are highly effective at removing Cd(II) across a wide pH range, significantly reducing its bioavailability and toxicity. Below a pH of 4.0, Cd(II) removal primarily occurs through ion exchange, in the pH range from 5.0 to 6.0, the predominant mechanisms are the formation of outer-sphere and inner-sphere complexes, at a pH of 6.0, Cd(II) binds to the (001) and (002) crystal faces of  $\delta$ -MnO<sub>2</sub> through surface complexation, forming triple corner-sharing (TCS) complexes, achieving a maximum adsorption capacity of

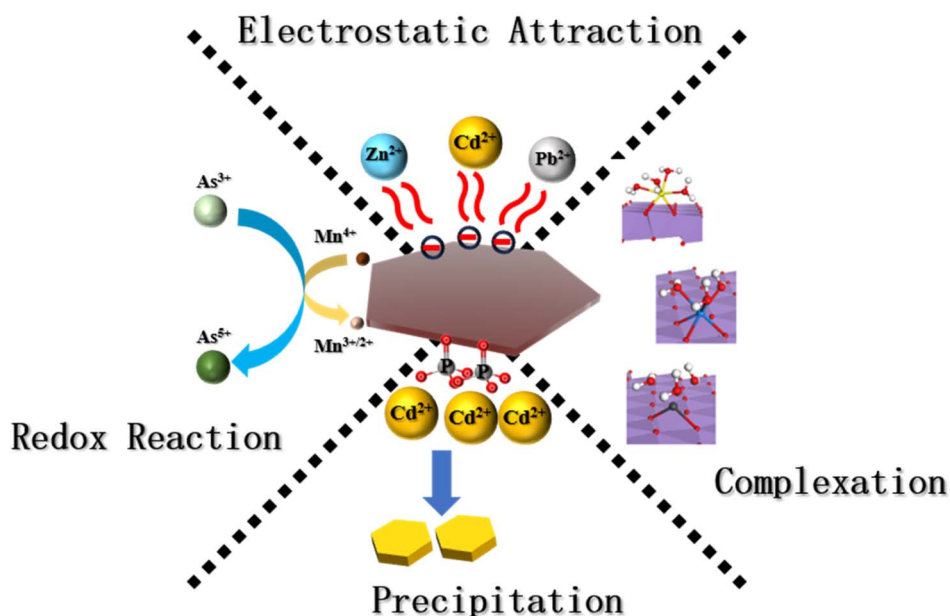


Fig. 1 Manganese oxide enrichment mode for different metal ions.

104.17 mg g<sup>-1</sup>.<sup>30–32</sup> Above a pH of 7.0, Cd(II) is completely adsorbed by MnO<sub>2</sub>.<sup>33</sup> The processes of Cd(II) removal through  $\delta$ -MnO<sub>2</sub> involve distinct mechanisms during adsorption and co-precipitation. In the adsorption process, Cd(II) interacts with layered manganese oxide (IV), whereas in co-precipitation, Mn(II) is oxidized to Mn(III) and forms double corner sharing (DCS) complex with Cd(II).<sup>34–36</sup> This detailed understanding of the interactions and conditions affecting Cd(II) removal enhances the potential for targeted remediation strategies in contaminated soils.

To enhance the adsorption capacity of manganese oxides for metal ions, researchers have developed innovative combinations with other adsorptive materials. Wang created a composite of todorokite and biochar (BRB), which demonstrated a remarkable adsorption capacity for Cd at 9068 mg kg<sup>-1</sup>, significantly surpassing that of birnessite alone at 4335 mg kg<sup>-1</sup>.<sup>18</sup> Xia improved the adsorptive properties of MnO<sub>2</sub> by incorporating yeast, finding that potassium permanganate (KMnO<sub>4</sub>) could alter the yeast's cell wall structure at pH values above 4.51, this alteration exposes more functional groups, like carboxyl and amino, enhancing the composite's capacity for Cd(II) adsorption.<sup>37–39</sup> Additionally, zeolite-loaded manganese oxide has been utilized as a soil amendment to promote the association of exchangeable Cd with manganese oxide, thereby bolstering the immobilization of Cd and reducing its uptake by plants. The use of this amendment led to significant reductions in Cd content in wheat grains, straw, and roots by 65.0%, 11.7%, and 55.3%, respectively.<sup>40,41</sup>

The adsorption mechanisms of manganese oxides involve spontaneous redox reactions;  $\delta$ -MnO<sub>2</sub>, for instance, can be reduced and dissolved by reductive substances. Qian explored combining  $\delta$ -MnO<sub>2</sub> with S<sup>2+</sup> and cysteine, revealing that S<sup>2+</sup> could relocate Cd(II) from vacancies to edge sites, forming CdS adsorbed on  $\delta$ -MnO<sub>2</sub> surfaces, at pH 5.5, cysteine induced the release of Cd(II) (52.8–68.6%) previously held in vacancies, while at pH 7.5, it facilitated the formation of Cd-cysteine complexes.<sup>6,42,43</sup> Wang reported maintaining a high removal efficiency of Cd at 96% at pH 5 with a thiosulfate/manganate (TS/Mn) molar ratio of 3, demonstrating the potential for tailored approaches to enhance heavy metal remediation in contaminated environments.<sup>44,45</sup> Furthermore, the reduction of Fe(II) to Mn(III) impacts Cd(II) adsorption on MnO<sub>2</sub> by shifting adsorption sites from vacancies to edge sites, forming DCS and double edge shared (DES) complexes. The introduction of new minerals, such as  $\beta$ -MnOOH and iron oxides, at pH 7.5 with Fe(II) resulted in weaker adsorption capabilities for Cd(II) compared to MnO<sub>2</sub>.<sup>46,47</sup>

These studies highlight how integrating manganese oxides with various materials can significantly boost their adsorption capacity for cadmium (Cd). This enhancement not only improves their effectiveness in controlling heavy metal pollution but also broadens their applicability in soil remediation efforts. Such advancements are crucial for developing more efficient strategies to mitigate the impact of heavy metals on the environment.

## 2.2 Enrichment of Pb by manganese oxides

Manganese oxides are particularly selective in their adsorption of metal ions, with  $\delta$ -MnO<sub>2</sub> demonstrating a preference for Pb

over Cu, Ni, and Zn, Pb to form stable Pb–O/OH bonds on the surface of  $\delta$ -MnO<sub>2</sub>, which enhances the stability of DES and TCS complexes, significantly increasing the adsorption selectivity for Pb.<sup>48</sup> A critical factor influencing this capacity is the Mn average oxidation state (MnAOS) of the oxides, as the MnAOS increases from 3.67 to 3.92, the maximum adsorption capacity for Pb correspondingly rises from 1320 to 2457 mmol kg<sup>-1</sup>.<sup>49,50</sup> X-ray photoelectron spectroscopy (XPS) analysis highlighted that used potassium permanganate (KMnO<sub>4</sub>) as a catalyst not only boosts the effectiveness of hydrated manganese dioxide (HMO) in removing Pb but also facilitates the oxidation of Pb(II) to Pb(IV) under alkaline conditions, in redox reaction, Mn(II) and Pb(IV) form Mn(OH)<sub>2</sub> and PbO<sub>2</sub>, respectively, with an oxidation efficiency for Pb(IV) reaching 50%.<sup>51</sup>

Manganese oxides already exhibit strong adsorptive properties for Pb. The strategic combination of manganese oxides with other materials further enhances this efficiency, creating composite materials with synergistic effects. These composites show great promise for the immobilization of Pb in various environmental applications.

For instance, a study produced manganese dioxide biochar (MBR) that demonstrated increased specific surface area and pore volume, XPS analysis identified the formation of Pb–O bonds or combinations with –OH groups as critical mechanisms for Pb(II) removal in MBR.<sup>52</sup> Wu developed a novel manganese dioxide modified biochar-based porous hydrogel (MBCG), this three-dimensional structure offers a uniform pore distribution and outstanding adsorptive performance, achieving a Pb adsorption capacity of 70.90 mg g<sup>-1</sup>, remarkably, MBCG also maintained an 80.5% adsorption efficiency after several recycling processes.<sup>53</sup> Layered double hydroxides (LDHs) and layered double oxides (LDOs) are celebrated for their ion-exchange and metal ion adsorption capabilities due to their anionic nature and robust thermal and chemical stability. Huang synthesized two materials, MnO<sub>2</sub>/MgFe-LDH and MnO<sub>2</sub>/MgFe-LDO, with Pb(II) adsorption primarily occurring through precipitation, functional group complexation, electrostatic attraction, cation exchange, isomorphic substitution, and memory effects. The MnO<sub>2</sub>/MgFe-LDO demonstrated exceptional regenerative adsorption capabilities, with an impressive adsorption capacity of 531.86 mg g<sup>-1</sup> for Pb(II).<sup>54</sup> Cui introduced a new MnO<sub>2</sub>@polyaniline (PANI) composite, showcasing enhanced adsorption capabilities for Pb(II) compared to the original materials, achieving over 99% removal efficiency at a dosage of 0.5 g L<sup>-1</sup>.<sup>55,56</sup>

Poly(*m*-phenylenediamine) (PmPD) has faced limitations as a heavy metal adsorbent due to its positively charged surface and small surface area. However, Xiong's innovative synthesis of MnO<sub>2</sub>@PmPD composites has demonstrated notable improvements. The key to these composites' enhanced performance lies in the oxidation products of aniline (a reducing group) present in PmPD, specifically quinone imine and carboxylate groups. These functional groups effectively bind with Pb(II). Through Density Functional Theory (DFT) analysis, it was determined that the (311) crystal plane of MnO<sub>2</sub>@PmPD serves as the primary adsorption site for Pb(II).<sup>65,66</sup>

Manganese oxides were combined with substances that possess adsorption capabilities, their ability to adsorb lead (Pb)



is significantly enhanced, this synergistic effect also can improve the capability of PmPD to address its deficiencies in metal adsorption. The application of manganese oxides, both individually and in conjunction with other adsorbents, offers substantial promise for effectively stabilizing lead in soil environments. This approach is crucial for reducing lead mobility and toxicity, contributing to safer and healthier soil ecosystems.

### 2.3 Enrichment of other metal elements by manganese oxides

Manganese oxides are highly effective in adsorbing various metal elements within the soil environment. Notably, Ni and Co could integrate into the structure of  $\delta$ -MnO<sub>2</sub> via isomorphic substitution, replacing Mn<sup>4+</sup> within its layers. However, Ni was effectively adsorbed onto the vacancies of the birnessite (001) surface, forming trigonal shared complexes that facilitated a removal rate of over 80% for Ni(II) at a pH of 7,<sup>67</sup> birnessite exhibited a marked increase in its adsorption capacity for Co(II) at pH 7.5, reaching about 280  $\mu\text{mol}/0.1\text{ g}$ , which was roughly double the capacity observed at pH 6.<sup>8,68</sup> Wu's research further revealed that the incorporation of Co(III) into manganese oxides resulted in a reduction of Mn(III) octahedra, which hindered the structural transition from layered to tunnel configurations.<sup>69</sup> The presence of Ni during the crystallization process of birnessite could inhibit the incorporation of Co, reducing the number of manganese layers in the co-doped mineral. This interaction demonstrated the competitive dynamics between Ni and Co within manganese oxide structures.<sup>48,70</sup>

Koppula explored NiCo(BDC)@MnO<sub>2</sub> composites maintained excellent stability at high temperatures and showcased remarkable adsorption capacities for Cu<sup>2+</sup> (756.82 mg g<sup>-1</sup>), Cr<sup>6+</sup> (111.22 mg g<sup>-1</sup>), and U<sup>6+</sup> (365.25 mg g<sup>-1</sup>).<sup>71</sup>

Zn(II) is absorbed onto acid birnessite and  $\delta$ -MnO<sub>2</sub> as endohedral complexes (Zn IV or Zn VI), which also decreases the Mn(III) content within the MnO<sub>x</sub> layers.<sup>72</sup> Interestingly, the adsorption rate for Zn(II) significantly increases from 36% to 96% as the pH value rises from 3 to 9.<sup>73</sup> Hawash's synthesis of two types of modified clinoptilolite, using Fe(III) and MnO<sub>2</sub>, demonstrated through Differential Thermal Analysis (DTA) that crystalline MnO<sub>2</sub>-clinoptilolite has a stronger adsorption capacity for Zn(II) compared to the amorphous Fe(III) clinoptilolite, reaching an efficiency of 99.65%.<sup>74</sup>

The removal of arsenic (As) varies depending on its oxidation state and the adsorption dynamics on the surfaces of metal oxides. Todorokite, for instance, can remove As with an efficiency of up to 98% within a pH range of 3 to 9. Wang revealed that As could be removed through endohedral complexes formed within the core-shell structure of MnO<sub>2</sub>@La(OH)<sub>3</sub>. Further enhancing the technology, Wen synthesized a MnO<sub>2</sub>-coated Fe<sub>3</sub>O<sub>4</sub> magnetic flower-like nanocomposite material, which achieved maximum adsorption capacities for As(III) and As(V) of 76.73 mg g<sup>-1</sup> and 120.50 mg g<sup>-1</sup>, respectively.<sup>75-77</sup>

Manganese can enter the soil through the deposition of throughfall or litterfall. Excessive uptake of soil manganese by plants, beyond their nutritional needs, can impair photosynthesis in species such as sugar maple and various flowers.<sup>78</sup>

Applying manganese can alter the soil's manganese content as well as the mobility and transformation of heavy metals. Table 2 details the study on the use of various manganese oxides and their composites to stabilize heavy metals in contaminated soils. By incorporating manganese oxide minerals and modified manganese materials, heavy metals can be concentrated in multiple ways (illustrated in Fig. 1) at different locations (shown in Fig. 2). These investigations underscore how manganese oxide minerals and their modified forms can significantly enrich metal elements through a variety of mechanisms at different sites. It has been noted that the valence state of manganese within these oxides plays a critical role in their capacity to enrich metals. Manganese oxides typically present in II/III/IV valence states, with divalent manganese often found in solution and serving as cations that adhere to manganese oxide minerals. This facilitates the transformation of manganese from lower to higher valence states, which subsequently impacts the behavior of heavy metal ions, either fixing or releasing them from manganese oxides.

The subsequent section will delve into the influence of low-valence Mn(II) on the adsorption of metal ions by manganese oxides. This exploration aims to further illuminate the diverse and potent capabilities of different manganese oxide forms to enrich metal ions, offering deeper insights into the mechanisms that govern their interactions and efficiencies in environmental remediation scenarios.

## 3 Impact of Mn(II) on manganese oxide enrichment of heavy metal

The varying oxidation states of manganese, particularly Mn(III) and Mn(IV), are essential for the catalytic efficiency of manganese oxides, previous studies have demonstrated that Mn(II) can alter the composition and structure of  $\delta$ -MnO<sub>2</sub> minerals.<sup>3</sup> A key process in the interaction of Mn(II) with manganese oxides is the comproportionation reaction, where Mn(II) and Mn(IV) combine to form two Mn(III).<sup>79</sup> This newly formed Mn(III) then undergoes disproportionation, reverting to Mn(II) and Mn(IV). This continuous cycle of reactions promotes the dynamic exchange among manganese different oxidation states, enhancing the reactivity and functional versatility of manganese oxides.<sup>80,81</sup> Higher pH levels facilitate the comproportionation and disproportionation reactions involving Mn(II),<sup>72,82</sup> when the pH exceeds 7.5 and Mn(II) is introduced, a noticeable transformation occurs in  $\delta$ -MnO<sub>2</sub>, transitioning to minerals like manganite ( $\gamma$ -Mn(III)OOH), feitknechtite ( $\beta$ -Mn(III)OOH), and hausmannite (Mn<sub>3</sub>O<sub>4</sub>), which have a greater capacity to stabilize Zn and Ni.<sup>11,12,83-85</sup> Research indicated that Mn(II) regulated the ability of manganese oxides to adsorb metal ions such as Co, Sb, and Cd.<sup>10,86-89</sup> This change underscores how pH and Mn(II) concentrations critically influence the structural development of manganese oxides. The changes in adsorption capacities resulted not only from structural modifications in the oxides but also from the role of Mn(II) in promoting the regeneration and transformation of manganese oxides into more reactive forms. This dynamic behavior emphasizes the complex



Table 2 Study on using various manganese oxides and their composites to stabilize heavy metals in contaminated soils

Manganese oxide material	Treatments	Effects	Reference
Amorphous manganese oxide (AMO)	Applied to agricultural soil contaminated by a smelting plant, adjust the pH to between 3 and 8	pH > 5, MnCO <sub>3</sub> forms on the surface of AMO, leading to reductions in the soil concentrations of As, Cu, Pb, and Sb to 20%, 35%, 7%, and 11% of their original levels, respectively	57
	AMO, Maghemite, and Magnetite were each applied to the soil surrounding a lead-copper smelting plant	After applying AMO, the concentrations of Cd, Cu, and Pb decreased by 92%, 92%, and 93%, respectively, which is an order of magnitude greater reduction compared to the other two materials used	58
Natural manganese oxide	Soil contaminated with Pb	After applying NMO, the soil showed a significant decrease in water-exchangeable Pb	59
Hydrous manganese oxides (HMO)	Sludge containing heavy metals and soil from around a smelting plant were used to simultaneously cultivate ryegrass and tobacco	HMO altered the binding of Cd and Pb in the soil, reducing their transfer from the soil to the soil solution and ultimately decreasing plant uptake of these heavy metals	60
Zeolite-loaded manganese oxide	Alkaline dryland soil containing Cd	The application reduced the available Cd content in the soil by 44.3% and increased the available Mn content by 61.9%	61
Fe–Mn modified biochar composite (FMBC)	Arsenic-contaminated paddy soil	FMBC application decreased the available arsenic content in the soil by promoting the transformation of non-specifically sorbed and specifically bound arsenic into residual forms and those bound to amorphous and crystalline hydrous oxides	62
Hiol-functionalized graphene oxide/Fe–Mn composite (SGO/Fe–Mn)	Soil contaminated with Hg	Applying 0.8% SGO/Fe–Mn can reduce the extractable mercury content by up to 98.9%	63
Birnessite	Soil contaminated with Cu	Birnessite lowered the free Cu <sup>2+</sup> activity in the soil	64

interactions within manganese oxides and their potential effectiveness in environmental remediation applications.

### 3.1 Mn(II) Facilitation of manganese oxide enrichment of metal elements

**3.1.1 Ni.** Ni adsorption on  $\delta$ -MnO<sub>2</sub> is relatively low, with only about 10% of Ni being adsorbed when the molar ratio of added Ni to  $\delta$ -MnO<sub>2</sub> is approximately 13, primarily because Ni tends to occupy manganese vacancies.<sup>25,67</sup> The interaction of pH and Mn(II) further affects Ni binding to manganese oxides.<sup>80,90,91</sup> At pH 6.5 and 4.0, Ni(II) is displaced from these vacancies by Mn(III), which is generated through Mn(II)-mediated comproportionation–disproportionation reactions, prompting Ni(II) to relocate from vacancy to edge sites, at pH 7.5, the presence of aqueous Mn(II) triggers the transformation of  $\delta$ -MnO<sub>2</sub> into secondary feitknechtite containing Ni(II), thereby increasing the removal rate of Ni(II) by approximately 30%.<sup>92</sup>

**3.1.2 Zn.** When  $\delta$ -MnO<sub>2</sub> adsorbed both Zn(II) and Mn(II), Mn(II) initially occupied the vacancies meant for Zn(II), prompting Zn(II) to shift from the vacancies of todorokite to edge sites.<sup>82,93</sup> This process was aided by the bio-oxidation of

manganese through surface ion exchange, which released Mn(II) oxidized by Mn(II) oxidase, thereby reducing the competitive adsorption between Mn(II) and Zn(II).<sup>94</sup> At pH 7.5, the interaction between Mn(II) and Zn(II) transformed todorokite into a spinel Zn(II)<sub>1-x</sub>Mn(II)<sub>x</sub>Mn(III)<sub>2</sub>O<sub>4</sub> precipitate, significantly increasing the adsorption capacities for Mn(II) and Zn(II) to 800  $\mu$ mol/0.1 g and 400  $\mu$ mol/0.1 g, respectively—eight and two times higher than at pH 6.5.<sup>82</sup> Moreover, Mn(II) triggered the formation of feitknechtite, manganite, and hausmannite from  $\delta$ -MnO<sub>2</sub>, with minimal Zn(II) precipitation in the solution. These newly formed minerals greatly enhanced the fixation of Zn(II).<sup>95</sup>

Mn(II), despite its strong competitive adsorption with Ni and Zn, can prompt the transformation of  $\delta$ -MnO<sub>2</sub> into feitknechtite and other tunnel-structured manganese oxides. This transformation enhances the stabilization of Ni and Zn within these structures.

### 3.2 Mn(II) inhibition of manganese oxide enrichment of metal elements

**3.2.1 Cd.** At a pH of 5.5, introducing Mn(II) at concentrations of 2 mM and 8 mM into a system containing  $\delta$ -MnO<sub>2</sub> adsorbing Cd(II) at 5 mM had led to a reduction in Cd(II)



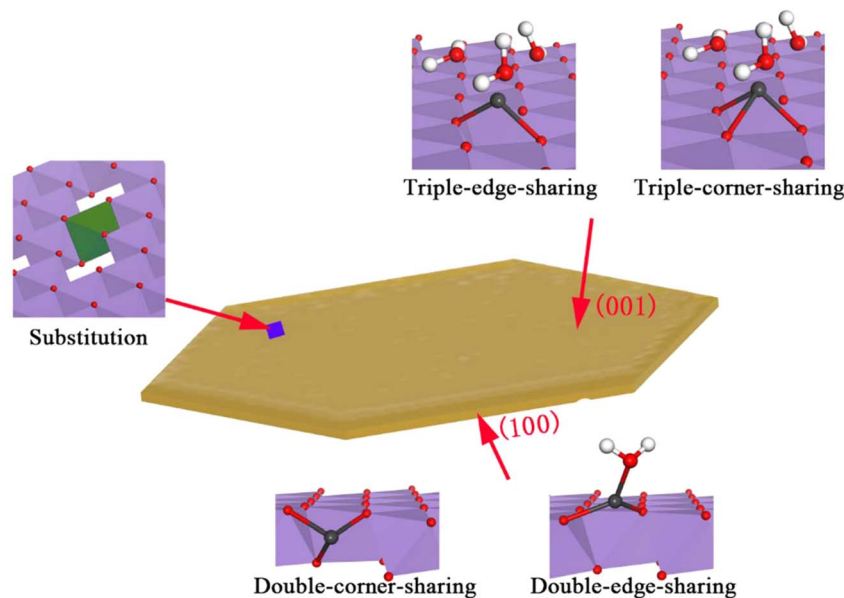


Fig. 2 Schematic representation of the different sites of enrichment of metallic elements by manganese oxide<sup>9,23</sup>

adsorption by approximately 10% and 20%, respectively.<sup>96</sup> To mitigate the inhibitory effect of Mn(II) on Cd(II) adsorption by  $\delta$ -MnO<sub>2</sub>, research had indicated that intermittent introduction of low concentrations of Mn(II) could effectively remove Mn with an efficiency of 97.40%, while causing minimal desorption of Cd(II), which had a release rate of only 0.73%, in contrast, adding high concentrations of Mn(II) directly had reacted with KMnO<sub>4</sub> to regenerate MnO<sub>2</sub>, providing a dual fixation effect that had enhanced the stabilization of Cd(II).<sup>97</sup> Natacha found that aeration treatments, which oxidized  $\beta$ -MnOOH and  $\delta$ -MnO<sub>2</sub>, had resulted in a decrease in pH and subsequent leaching of Cd(II). On the other hand, anoxic treatments had helped prevent some Mn(II) from oxidizing into MnSiO<sub>3</sub> and Mn(II)Al-LDH, thereby better stabilizing Cd(II).<sup>98</sup>

**3.2.2 Co.** For Co(II), it could substitute Mn(II) within the secondary  $\beta$ -Mn(III)OOH lattice formed during the reaction between Mn(II) and  $\delta$ -MnO<sub>2</sub>, thereby inhibiting the adsorption and reductive transformation of Mn(II) on  $\delta$ -MnO<sub>2</sub>.<sup>92</sup> At a pH of 7.5, the introduction of Mn(II) (1 mM) had facilitated the reductive transformation of isomorphically substituted Co(III) in  $\delta$ -MnO<sub>2</sub> (0.1 g/L), leading to the formation of feitknechtite containing Co(II), with some Co(II) being released into the solution.<sup>8</sup>

**3.2.3 Sb.** Antimony (Sb), a toxic and carcinogenic element, was found in trace amounts in natural environments, typically in the oxidation states Sb(III) and/or Sb(V).<sup>99</sup> Previous research had demonstrated that manganese oxides played a crucial role in regulating antimony in soils and sediments. Sb was adsorbed onto the edge sites of manganese oxides through coprecipitation, forming endohedral complexes with an adsorption capacity of up to 342.0  $\mu\text{mol g}^{-1}$ .<sup>100–103</sup> In a pH 7.5  $\delta$ -MnO<sub>2</sub> coprecipitation system with Sb, the addition of 10 mM Mn(II) had transformed  $\delta$ -MnO<sub>2</sub> into manganite and hausmannite within 24 hours, resulting in a composition of 93% and 7%,

respectively, the released Mn(II) concentration was around 5 mM, while the release of Sb was almost undetectable.<sup>104</sup>

Additionally, Sb(V) significantly affected the Mn(II)-induced transformation of  $\delta$ -MnO<sub>2</sub>. At varying concentrations of aqueous Sb(V) (low: 10  $\mu\text{mol L}^{-1}$ , medium: 200  $\mu\text{mol L}^{-1}$ , and high: 600  $\mu\text{mol L}^{-1}$ ),  $\delta$ -MnO<sub>2</sub> was transformed into manganite, hausmannite, and groutite ( $\alpha$ -Mn(III)OOH). The removal efficiencies for Sb at these concentrations were 85%, 28%, and 14%, respectively, with the released Mn(II) concentration stabilizing at approximately 2.7  $\text{mmol L}^{-1}$ .<sup>105</sup>

These studies highlighted the intricate interactions between Mn(II) and other metal ions in the presence of manganese oxides, demonstrating that Mn(II) could either facilitate or hinder metal adsorption during the transformation of todorokite into other manganese oxide minerals. This transformation was influenced by several factors, including pH, Mn(II) concentration, and the presence of competing metal ions. Such processes were vital for regulating the mobility of heavy metals, as Mn(II) played a key role in the structural and morphological evolution of manganese oxides within the soil environment. Understanding these dynamic interactions is crucial for managing the geochemical behavior of heavy metals in contaminated soils, offering valuable insights for environmental remediation and pollution control strategies.

## 4 Interaction between manganese oxides and soil components

Soil, as the most frequently interacted-with layer in human activities, contains a diverse array of minerals and reactive substances formed through sedimentary processes. These soil components mutually influence each other's migration and transformation. Manganese oxide minerals play a key role in the removal and transformation of organic materials, humic

substances, and oxyanions within the soil.<sup>16</sup> Conversely, these soil components can also impact the structure and functionality of manganese oxides, leading to complex and interdependent interactions between them.

#### 4.1 Potential of manganese oxides for organic matter degradation and stabilization

Manganese was a highly reactive component in soil, actively participating in the removal and transformation of organic matter through redox reactions under both aerobic and anaerobic conditions, making it a key player in carbon sequestration.<sup>106–109</sup> The primary mechanism by which manganese oxides adsorbed organic matter mirrored their role in heavy metal removal, relying on electrostatic interactions.<sup>109</sup> In neutral environments, manganese oxides carried a negative charge, allowing them to adsorb positively charged functional groups, such as those in proteins.<sup>110</sup>

The adsorption of organic matter on manganese oxide surfaces was influenced by the specific functional groups present.<sup>111</sup> Organic compounds containing hydrophobic groups and nitrogen tended to be more readily adsorbed onto manganese oxides.<sup>112,113</sup> Additionally, high molecular weight organic compounds with aromatic structures were preferentially adsorbed and were more likely to undergo oxidation, breaking down into lower molecular weight compounds.<sup>114</sup> This selective adsorption and transformation of organic matter by manganese oxides played a crucial role in the cycling and stabilization of organic carbon in soils.

In the context of organic pollutant removal, it was essential to consider both the degradation of these pollutants and the fixation of carbon. Research had shown that during the removal of organic matter by various manganese oxide minerals, dissolved oxygen oxidized Mn(II) to Mn(III), which induced the transformation of  $\delta$ -MnO<sub>2</sub> into minerals such as feitknechtite, manganite, and hausmannite, however, the formation of Mn(III) could block active sites on the manganese oxides, thereby reducing the oxidation of phenol and ultimately inhibiting its degradation.<sup>115</sup> Additionally, oxygen competed with fulvic acid (FA) for active sites on MnO<sub>2</sub>, making anaerobic conditions more effective for removing total organic carbon (TOC), achieving removal rates as high as 79.8%, the transformation of  $\delta$ -MnO<sub>2</sub> into MnOOH could also lead to the preservation of organic carbon by producing insoluble MnCO<sub>3</sub> crystals.<sup>87,116–119</sup>

Humification was another crucial process, significantly influencing the physicochemical properties of soil and supporting plant growth and development.<sup>119</sup> Manganese oxides, with their high redox potential, held promise for enhancing humification processes. MnO<sub>2</sub> and its reduction products (MnOOH and Mn(II)) could catalyze the reduction of fulvic-like acids (FLAs) and humic-like acids (HLAs), leading to the production of CO<sub>2</sub>.<sup>120</sup> Research by Qi found that  $\delta$ -MnO<sub>2</sub> could catalyze the further condensation of unstable substances into highly aromatic complex substances, thereby increasing the degree of humification of FA and improving the bioavailability of HLAs.<sup>17,121</sup> Similarly, Li's research on methanol oxidation using Mn<sub>2</sub>O<sub>3</sub> and  $\delta$ -MnO<sub>2</sub> revealed that the

comproportionation–disproportionation reactions within these manganese oxides could enhance lattice oxygen transfer and Mn(IV) oxidation, thereby boosting the efficiency of methanol oxidation.<sup>122</sup> These findings underscored the multifaceted role of manganese oxides in both pollutant degradation and the enhancement of soil organic matter stability.

These studies illustrate the significant role of manganese oxides in the removal of organic substances and in the transformation and fixation of carbon, underlining their importance in soil management and environmental remediation strategies.

#### 4.2 Influence of cations and anions on the structure and functionality of manganese oxides

**4.2.1 Cationic.** In soil environments, the presence of cations had a profound impact on the structure of manganese oxides, and these structural changes, in turn, affected their adsorption and oxidation capabilities. For example, Na(I) and Ca(II) promoted the formation of Mn(III) and its orderly distribution within the Mn octahedral layers. Conversely, H(I) and Ni(II) led to the creation of vacancies, which enhanced the competitive adsorption of Ni(II) and Mn(II) at these sites.<sup>123</sup> Additionally, increasing concentrations of K(I) increased the amount of mobile oxygen on the surface of MnO<sub>2</sub>, thereby boosting the oxidative activity of  $\delta$ -MnO<sub>2</sub> toward formaldehyde (HCHO).<sup>124</sup>

The presence of NH<sub>4</sub><sup>+</sup> in mineral resource utilization presented challenges due to its removal difficulty and the potential for secondary pollution. Numerous studies had investigated the transformation and removal processes of NH<sub>4</sub><sup>+</sup> within manganese oxide minerals, revealing that the average oxidation state of manganese (MnAOS) and pH were critical factors in its transformation and removal.<sup>125</sup> NH<sub>4</sub><sup>+</sup> was more readily released under alkaline conditions than under acidic ones, with electrostatic interactions and ion exchange between OH<sup>-</sup> and NH<sub>4</sub><sup>+</sup> being the primary mechanisms for its removal. NH<sub>4</sub><sup>+</sup> could be oxidized by Mn(IV) to NO<sub>3</sub><sup>-</sup> and N<sub>2</sub>, with Mn present in forms such as MnO<sub>2</sub>, Mn<sub>2</sub>O<sub>3</sub>, MnOOH, and Mn<sub>3</sub>O<sub>4</sub>.<sup>126–128</sup> The removal rate of NH<sub>4</sub><sup>+</sup> was also influenced by coexisting cations in the solution, with the effectiveness ranking as Ca<sup>2+</sup> > K<sup>+</sup> > Mg<sup>2+</sup> > Na<sup>+</sup>.<sup>129</sup>

**4.2.2 Oxygenated anion.** Oxygenated anion in soil played a crucial role in regulating the crystalline growth of manganese oxides and their ability to degrade various substances. Research had shown that oxyanions such as phosphate, sulfate, and silicate could adsorb at the edge sites of MnO<sub>6</sub> octahedra, thereby inhibiting the lateral growth of the MnO<sub>6</sub>(100) crystal face, with phosphate exerting the most significant influence.<sup>14,130</sup> The interactions between these oxyanions and manganese could mutually affect the binding capabilities of manganese oxides. Negatively charged polycarboxylic compounds tended to bind preferentially at edge sites, which enhanced the stabilization ability of  $\delta$ -MnO<sub>2</sub> for Mn(III).<sup>109,131–134</sup> Additionally, the involvement of Mn(II) in proton exchange could reduce the negative surface charge of MnO<sub>2</sub>, thereby increasing its capacity to remove oxyanions such as phosphate and silicate.<sup>85</sup>



The adsorption of sulfate ( $\text{SO}_4^-$ ) and hydroxyl radicals ( $\cdot\text{OH}$ ) on manganese oxides could also facilitate the degradation of organic substances.<sup>135</sup> Density Functional Theory (DFT) calculations had indicated that the  $\alpha$ - $\text{MnO}_2$  (211 crystal face) could more effectively activate peroxymonosulfate (PMS), leading to the generation of  $\text{SO}_4^-$  and  $\cdot\text{OH}$  radicals. Consequently, manganese oxides with higher crystallinity, such as  $\alpha$ -,  $\beta$ -, and  $\gamma$ - $\text{MnO}_2$ , exhibited stronger capabilities for degrading organic materials compared to  $\delta$ - $\text{MnO}_2$ .<sup>136,137</sup>

These findings underscore the complex chemistry between manganese oxides and both cations and anions in soil, which profoundly impacts their environmental roles and their applications in soil remediation and management.

### 4.3 Microbial promotion of the manganese cycle

Microorganisms, including bacteria, fungi, algae, and diatoms, played a crucial role in biogeochemical cycles through a variety of enzymatic and non-enzymatic pathways.<sup>138</sup> As key components of the soil ecosystem, these microorganisms significantly influenced the mineralization processes of natural manganese oxides.<sup>139</sup> Microbes utilized enzymes to promote the production of extracellular superoxide radicals (in bacteria) and reactive oxygen species (in fungi and algae), which indirectly oxidized  $\text{Mn(II)}$  to  $\text{Mn(III)}$ , through comproportionation–disproportionation reactions, these processes generated  $\text{Mn(II)}$  and  $\text{Mn(IV)}$ , with superoxide-producing microbes potentially serving as key drivers of mineral formation and transformation in soil environments.<sup>140–142</sup> The microbial mediation of mineralization could occur at the micrometer scale and proceeded at a high rate, highlighting the significant role of bacteria and fungi in the reduction of  $\text{Mn(IV)}$ .<sup>143</sup>

Microorganisms indirectly participated in the mineralization of  $\text{Mn(II)}$  and the reduction of  $\text{Mn(IV)}$ , acting as catalytic agents that drove the cycling of manganese across various oxidation states within the environment.<sup>144</sup> This microbial activity not only facilitated the transformation and cycling of manganese but also enhanced the biogeochemical cycling of other essential nutrients and metals within the soil, thereby contributing to soil fertility and overall ecosystem functioning.

## 5 Conclusions and future perspective

Manganese oxides play a crucial role in maintaining the normal operation of the soil layer. They act as catalysts for redox reactions, which are vital for nutrient cycling and the degradation of contaminants. Manganese oxides can oxidize organic contaminants and reduce potentially toxic metal ions, thereby mitigating their mobility and bioavailability in the soil environment. Their high reactivity also allows manganese oxides to interact with soil organic matter, leading to the formation of stable organo–mineral complexes that can sequester carbon and metals, further influencing soil fertility and structure.

Additionally, manganese oxides can interact with other soil minerals to affect soil pH, electrochemical properties, and cation exchange capacity, all of which are fundamental to soil

health and plant growth. The presence of manganese oxides can also enhance the microbial degradation of organic compounds by serving as electron acceptors, thereby promoting biogeochemical cycles within the soil.

Thus, understanding the interactions between manganese oxides and soil components is essential for developing strategies for soil management and remediation, as well as for predicting the environmental fate of pollutants in the soil matrix. These interactions highlight the importance of manganese oxides in environmental geochemistry and their potential applications in sustainable agriculture and environmental protection.

## Data availability

This article is a review and does not contain any new data. All information is derived from previously published articles, which are cited accordingly in the reference section. Data sharing is not applicable to this article as no new data were created or analyzed in this study. All data discussed are from previously published research articles.

## Conflicts of interest

The authors have declared there exist no competing interests.

## Acknowledgements

Thanks to the support of Yunnan Provincial Basic Research Program No. 202201AU070178, Yunnan Agricultural University Research Initiation Project No. F2022-07, The National Natural Science Foundation of China No. 42367005, Yunnan Fundamental Research Projects No. 202301AU070122, 202401AT070044 and Yunnan Academy of Agricultural Sciences pre-research project No. 2024KYZX-04.

## References

- 1 M. Sathish, C. L. Peacock, S. Franziska, G. Anja, M. Dirk, K. Erika and B. Georg, *Chem. Geol.*, 2015, **402**, 6–17.
- 2 D. Gasparatos, *Environ. Chem. Lett.*, 2013, **11**, 1–9.
- 3 E. J. Elzinga, *Environ. Sci. Technol.*, 2011, **45**, 6366–6372.
- 4 X. H. Feng, L. M. Zhai, W. F. Tan, F. Liu and J. Z. He, *Environ. Pollut.*, 2006, **147**, 366–373.
- 5 L. D. Puppa, M. Komárek, F. Bordas, J.-C. Bollinger and E. Joussein, *J. Colloid Interface Sci.*, 2013, **399**, 99–106.
- 6 A. A. Simanova, K. D. Kwon, S. E. Bone, J. R. Bargar, K. Refson, G. Sposito and J. Peña, *Geochim. Cosmochim. Acta*, 2015, **164**, 191–204.
- 7 Q. Wang, P. Yang and M. Zhu, *Geochim. Cosmochim. Acta*, 2019, **250**, 292–310.
- 8 Z. Huaiyan, F. Xionghan, L. Sungsik, R. Benjamin and E. J. Elzinga, *Chem. Geol.*, 2023, **618**, 121281.
- 9 H. Yin, J. Sun, X. Yan, X. Yang, X. Feng, W. Tan, G. Qiu, J. Zhang, M. Ginder-Vogel and F. Liu, *Environ. Pollut.*, 2020, **256**, 113462.





- 10 Z. Huaiyan, Z. Mengqiang, L. Wei, E. E. J. V. Mario, L. Fan, Z. Jing, F. Xionghan and S. D. L, *Environ. Sci. Technol.*, 2016, **50**, 1750–1758.
- 11 J. P. Lefkowitz, A. A. Rouff and E. J. Elzinga, *Environ. Sci. Technol.*, 2013, **47**, 10364–10371.
- 12 Y. Peng, W. Ke, B. K. A, X. Wenqian, W. Qian, M. Dong, W. Juan and Z. Mengqiang, *Environ. Sci. Technol.*, 2021, **55**, 3419–3429.
- 13 P. Jaya and P. Tarasankar, *Nanoscale*, 2015, **7**, 14159–14190.
- 14 W. Qian, L. Xianya, X. Wenqian, R. Yang, K. J. Livi and Z. Mengqiang, *Inorg. Chem.*, 2016, **55**, 10248–10258.
- 15 G. R. Aiken, H.-K. Heileen and J. N. Ryan, *Environ. Sci. Technol.*, 2011, **45**, 3196–3201.
- 16 K. Markus, I. C. Bourg, E. K. Coward, C. M. Hansel, S. C. B. Myneni and N. Naoise, *Nat. Rev. Earth Environ.*, 2021, **2**, 402–421.
- 17 O. W. Moore, C. Lisa, W. Clare, J. A. Bradley, B. Peyman, B. J. W. Mills, W. B. Homoky, X. KeQing, A. W. Bray, B. J. Fisher, K. Majid, K. Burkhard, A. W. Dale and C. L. Peacock, *Nature*, 2023, **621**, 312–317.
- 18 H. Wang, C. Peng, Z. Yong-Guan, C. Kuang and S. Guo-Xin, *Environ. Sci. Pollut. Res. Int.*, 2019, **26**, 8575–8584.
- 19 S. F. Qing, C. J. Dong, T. Zhong, L. W. Ju, H. X. Yuan and Z. F. Jie, *Plant Soil*, 2018, **433**, 377–389.
- 20 X. Liang, J. E. Post, B. Lanson, X. Wang, M. Zhu, F. Liu, W. Tan, X. Feng, G. Zhu, X. Zhang and J. J. D. Yoreo, *Environ. Sci.: Nano*, 2019, **7**, 238–249.
- 21 M. Villalobos, B. Toner, J. Bargar and G. Sposito, *Geochim. Cosmochim. Acta*, 2003, **67**, 2649–2662.
- 22 J. E. Post, *Proc. Natl. Acad. Sci. U. S. A.*, 1999, **96**, 3447–3454.
- 23 K. D. Kwon, K. Refson and G. Sposito, *Geochim. Cosmochim. Acta*, 2013, **101**, 222–232.
- 24 M. Alain and S. N. Steinmann, *ACS Earth Space Chem.*, 2021, **5**, 66–76.
- 25 C. A. J. Appelo and D. Postma, *Geochim. Cosmochim. Acta*, 2000, **64**, 3931.
- 26 G. Lee, J. M. Bigham and G. Faure, *Appl. Geochem.*, 2002, **17**, 569–581.
- 27 Å. Agneta, B. Lars, B. I. A, N. G. F, N. Monica and S. Staffan, *Environ. Health Perspect.*, 2014, **122**, 431–438.
- 28 Z. Lingxiao, G. Cheng, C. Chuan, Z. Wenwen, H. Xin-Yuan and Z. Fang-Jie, *Environ. Sci. Technol.*, 2020, **54**, 10100–10108.
- 29 R. Liu, H. Liu, Z. Qiang, J. Qu, G. Li and D. Wang, *J. Colloid Interface Sci.*, 2008, **331**, 275–280.
- 30 C. L. Chen and X. K. Wang, *Appl. Geochem.*, 2007, **22**, 436–445.
- 31 K. Eun-Ju, L. Chung-Seop, C. Yoon-Young and C. Yoon-Seok, *ACS Appl. Mater. Interfaces*, 2013, **5**, 9628–9634.
- 32 X. Huang, T. Chen, X. Zou, M. Zhu, D. Chen and M. Pan, *Int. J. Environ. Res. Public Health*, 2017, **14**, 1145.
- 33 M. I. Zaman, S. Mustafa, S. Khan and B. Xing, *J. Colloid Interface Sci.*, 2009, **330**, 9–19.
- 34 S. Kohei, K. Tatsuya, F. Shigeshi and T. Chiharu, *Chem. Geol.*, 2020, **550**, 119744.
- 35 A. A. Mamun, M. Morita, M. Matsuoka and C. Tokoro, *J. Hazard. Mater.*, 2017, **334**, 142–149.
- 36 Y. Wang, X. Feng, M. Villalobos, W. Tan and F. Liu, *Chem. Geol.*, 2012, **292–293**, 25–34.
- 37 Y. Zhang, J. Zhu, L. Zhang, Z. Zhang, M. Xu and M. Zhao, *Desalination*, 2011, **278**, 42–49.
- 38 Y. Xia, L. Meng, Y. Jiang, Y. Zhang, X. Dai and M. Zhao, *Chem. Eng. J.*, 2015, **259**, 927–935.
- 39 Y. Ren, N. Yan, Q. Wen, Z. Fan, T. Wei, M. Zhang and J. Ma, *Chem. Eng. J.*, 2011, **175**, 1–7.
- 40 J. Lin, Y. Zhan, Z. Zhu and Y. Xing, *J. Hazard. Mater.*, 2011, **193**, 102–111.
- 41 W. Weihua, L. Tao, L. Lihu, Y. Xiong, S. Xuecheng, Q. Guohong, H. Dangling and Z. Dongmei, *J. Hazard. Mater.*, 2021, **419**, 126464.
- 42 Q. Sun, P.-X. Cui, M. Zhu, T.-T. Fan, S. T. Ata-Ul-Karim, J.-H. Gu, S. Wu, D.-M. Zhou and Y.-J. Wang, *Environ. Int.*, 2019, **130**, 104932.
- 43 S. Qian, C. Peixin, W. Song, L. Cun, F. Tingting, A. M. Eduardo, C. Hu, H. Meiying, Z. Dongmei and W. Yujun, *Environ. Sci. Technol.*, 2020, **54**, 14955–14963.
- 44 P. Wang, H. Cheng, J. Ding, J. Ma, J. Jiang, Z. Huang, J. Li, S. Pang, C. Guan and Y. Gao, *Chem. Eng. J.*, 2020, **380**, 122585.
- 45 Y. Liu, L. Wang, X. Wang, Z. Huang, C. Xu, T. Yang, X. Zhao, J. Qi and J. Ma, *Water Res.*, 2017, **124**, 149–157.
- 46 C. M. van Genuchten and J. Peña, *Environ. Sci.: Processes Impacts*, 2016, **18**, 1030–1041.
- 47 Q. Sun, P. X. Cui, T. T. Fan, S. Wu, M. Zhu, M. E. Alves, D. M. Zhou and Y. J. Wang, *Chem. Eng. J.*, 2018, **353**, 167–175.
- 48 A. Manceau, M. Lanson and Y. Takahashi, *Am. Mineral.*, 2014, **99**, 2068–2083.
- 49 W. Zhao, W. Tan, M. Wang, J. Xiong, F. Liu, L. Weng and L. K. Koopal, *Environ. Sci. Technol.*, 2018, **52**, 10522–10531.
- 50 W. Zhao, X. Feng, W. Tan, F. Liu and S. Ding, *J. Environ. Sci.*, 2009, **21**, 520–526.
- 51 X. Qi and F. C. Xie, *Chem. Eng. J.*, 2018, **351**, 22–30.
- 52 J. Liang, X. M. Li, Z. G. Yu, G. M. Zeng, Y. Luo, L. B. Jiang, Z. X. Yang, Y. Y. Qian and H. P. Wu, *ACS Sustainable Chem. Eng.*, 2017, **5**, 5049–5058.
- 53 Z. Y. Wu, X. X. Chen, B. L. Yuan and M. L. Fu, *Chemosphere*, 2020, **239**, 124745.
- 54 Y. X. Huang, X. P. Luo, C. M. Liu, S. H. You, S. Rad and L. T. Qin, *RSC Adv.*, 2023, **13**, 19288–19300.
- 55 C. Cui, X. H. Sun, C. Q. Zhou, Y. W. Liu, H. X. Xiong, Y. N. Li and J. Han, *Colloids Surf., A*, 2021, **616**, 126336.
- 56 J. Han, J. Dai and R. Guo, *J. Colloid Interface Sci.*, 2011, **356**, 749–756.
- 57 V. Ettler, Z. Tomášová, M. Komárek, M. Mihaljevic, O. Sebek and Z. Michálková, *J. Hazard. Mater.*, 2015, **286**, 386–394.
- 58 Z. Michálková, M. Komárek, H. Sillerová, L. Della Puppa, E. Joussein, F. Bordas, A. Vanek, O. Vanek and V. Ettler, *J. Environ. Manage.*, 2014, **146**, 226–234.
- 59 C. M. McCann, N. D. Gray, J. Tourney, R. J. Davenport, M. Wade, N. Finlay, K. A. Hudson-Edwards and K. L. Johnson, *Chemosphere*, 2015, **138**, 211–217.
- 60 M. J. Mench, V. L. Didier, M. Löffler, A. Gomez and P. Masson, *J. Environ. Qual.*, 1994, **23**, 58–63.



- 61 W. Wang, T. Lu, L. Liu, X. Yang, X. Sun, G. Qiu, D. Hua and D. Zhou, *J. Hazard. Mater.*, 2021, **419**, 126464.
- 62 L. N. Lin, Z. Y. Li, X. W. Liu, W. W. Qiu and Z. G. Song, *Environ. Pollut.*, 2019, **244**, 600–607.
- 63 Y. Huang, M. Wang, Z. Li, Y. Gong and E. Y. Zeng, *J. Hazard. Mater.*, 2019, **373**, 783–790.
- 64 M. B. McBride and C. E. Martínez, *Environ. Sci. Technol.*, 2000, **34**, 4386–4391.
- 65 T. Xiong, X. Z. Yuan, H. Wang, L. B. Jiang, Z. B. Wu, H. Wang and X. Y. Cao, *J. Hazard. Mater.*, 2020, **389**, 122154.
- 66 T. Rong, L. Qin, D. Liang, C. Hao and Z. Jianping, *Environ. Technol.*, 2012, **33**, 341–348.
- 67 C. L. Peacock and D. M. Sherman, *Chem. Geol.*, 2006, **238**, 94–106.
- 68 P. Yang, J. W. Wang, S. Wang, C. Y. Yang, P. Y. Zhao, B. F. Huang, Q. Wang and H. F. Wang, *ACS Omega*, 2022, **7**, 37452–37464.
- 69 Z. K. Wu, C. L. Peacock, B. Lanson, H. Yin, L. R. Zheng, Z. J. Chen, W. F. Tan, G. H. Qiu, F. Liu and X. H. Feng, *Geochim. Cosmochim. Acta*, 2019, **246**, 21–40.
- 70 H. Yin, H. Li, Y. Wang, M. Ginder-Vogel, G. H. Qiu, X. H. Feng, L. R. Zheng and F. Liu, *Chem. Geol.*, 2014, **381**, 10–20.
- 71 S. Koppula, P. Jagasia, M. K. Panchangam and S. B. M. Surya, *J. Solid State Chem.*, 2022, **312**, 123168.
- 72 S. L. Zhao, Q. Wang, J. Y. Sun, O. J. Borkiewicz, R. X. Huang, E. M. Saad, B. Fields, S. Chen, M. Q. Zhu and Y. Z. Tang, *Chem. Geol.*, 2018, **493**, 234–245.
- 73 Z. Wang, C. Peacock, K. D. Kwon, X. Y. Gu, X. H. Feng and W. Li, *Geochim. Cosmochim. Acta*, 2023, **348**, 68–84.
- 74 H. B. I. Hawash, E. Chmielewska, Z. Netriová, J. Majzlan, H. Pálková, P. Hudec and R. Sokolík, *J. Environ. Chem. Eng.*, 2018, **6**, 6489–6503.
- 75 Y. L. Wang, C. Guo, L. Zhang, X. H. Lu, Y. H. Liu, X. H. Li, Y. Y. Wang and S. F. Wang, *Int. J. Environ. Res. Public Health*, 2022, **19**, DOI: [10.3390/ijerph191710649](https://doi.org/10.3390/ijerph191710649).
- 76 Y. Zhang, B. C. Zhao, C. J. Wang, Y. Y. Huang, X. Liu, R. K. Wang and C. B. Wang, *J. Hazard. Mater.*, 2023, **459**, 132079.
- 77 Z. P. Wen, Y. L. Zhang, Y. Wang, L. N. Li and R. Chen, *Chem. Eng. J.*, 2017, **312**, 39–49.
- 78 S. B. Horsley, R. P. Long, S. W. Bailey, R. A. Hallett and T. J. Hall, *Can. J. For. Res.*, 2000, **30**, 1365–1378.
- 79 J. R. Bargar, B. M. Tebo, U. Bergmann, S. M. Webb, P. Glatzel, V. Q. Chiu and M. Villalobos, *Am. Mineral.*, 2015, **90**, 143–154.
- 80 E. J. Elzinga and A. B. Kustka, *Environ. Sci. Technol.*, 2015, **49**, 4310–4316.
- 81 E. J. Elzinga, *Environ. Sci. Technol.*, 2016, **50**, 8670–8677.
- 82 J. P. Lefkowitz and E. J. Elzinga, *Environ. Sci. Technol.*, 2015, **49**, 4886–4893.
- 83 Q. Wang, P. Yang and M. Q. Zhu, *Geochim. Cosmochim. Acta*, 2019, **250**, 292–310.
- 84 P. Yang, S. Lee, J. E. Post, H. F. Xu, Q. Wang, W. Q. Xu and M. Q. Zhu, *Geochim. Cosmochim. Acta*, 2018, **240**, 173–190.
- 85 Q. Z. Li, R. Pokharel, L. Zhou, M. Pasturel and K. Hanna, *Environ. Sci.: Nano*, 2020, **7**, 4022–4031.
- 86 M. A. G. Hinkle, E. D. Flynn and J. G. Catalano, *Geochim. Cosmochim. Acta*, 2016, **192**, 220–234.
- 87 J. E. Johnson, P. Savalia, R. Davis, B. D. Kocar, S. M. Webb, K. H. Nealson and W. W. Fischer, *Environ. Sci. Technol.*, 2016, **50**, 4248–4258.
- 88 E. Silvester, A. Manceau and V. A. Drits, *Am. Mineral.*, 2015, **82**, 962–978.
- 89 D. R. Learman, S. D. Wankel, S. M. Webb, N. Martinez, A. S. Madden and C. M. Hansel, *Geochim. Cosmochim. Acta*, 2011, **75**, 6048–6063.
- 90 A. Manceau, C. Tommaseo, S. Rihs, N. Geoffroy, D. Chateigner, M. Schlegel, D. Tisserand, M. A. Marcus, N. Tamura and Z.-S. Chen, *Geochim. Cosmochim. Acta*, 2005, **69**, 4007–4034.
- 91 M. A. Marcus, A. Manceau and M. Kersten, *Geochim. Cosmochim. Acta*, 2004, **68**, 3125–3136.
- 92 J. P. Lefkowitz and E. J. Elzinga, *Chem. Geol.*, 2017, **466**, 524–532.
- 93 M. A. G. Hinkle, K. G. Dye and J. G. Catalano, *Environ. Sci. Technol.*, 2017, **51**, 3187–3196.
- 94 J. N. Chang, Y. Tani, H. Naitou, N. Miyata, F. Tojo and H. Seyama, *Chem. Geol.*, 2014, **383**, 155–163.
- 95 S. L. Zhao, Y. A. González-Valle, E. J. Elzinga, E. M. Saad and Y. Z. Tang, *Chem. Geol.*, 2018, **492**, 12–19.
- 96 Q. Sun, P. X. Cui, M. Zhu, T. T. Fan, S. T. Ata-Ul-Karim, J. H. Gu, S. Wu, D. M. Zhou and Y. J. Wang, *Environ. Int.*, 2019, **130**, 104932.
- 97 J. Zhang and F. C. Xie, *Environ. Sci. Pollut. Res.*, 2022, **29**, 36295–36312.
- 98 N. Van Groeningen, I. Christl and R. Kretzschmar, *Environ. Sci. Technol.*, 2021, **55**, 1650–1658.
- 99 M. Filella, N. Belzile and Y. W. Chen, *Earth-Sci. Rev.*, 2002, **57**, 125–176.
- 100 X. Wang, M. He, C. Lin, Y. Gao and L. Zheng, *Geochemistry*, 2012, **72**, 41–47.
- 101 Q. Sun, C. Liu, M. E. Alves, S. T. Ata-Ul-Karim, D. M. Zhou, J. Z. He, P. X. Cui and Y. J. Wang, *J. Eng.*, 2018, 473, DOI: [10.1016/j.cej.2018.02.091](https://doi.org/10.1016/j.cej.2018.02.091).
- 102 N. Belzile, Y.-W. Chen and Z. Wang, *Chem. Geol.*, 2001, **174**, 379–387.
- 103 X. Sun, B. Li, F. Han, E. Xiao, Q. Wang, T. Xiao and W. Sun, *Environ. Pollut.*, 2019, **252**, 1872–1881.
- 104 N. Karimian, S. G. Johnston and E. D. Burton, *J. Hazard. Mater.*, 2021, **404**, 124227.
- 105 N. Karimian, K. Hockmann, B. Planer-Friedrich, S. G. Johnston and E. D. Burton, *Environ. Sci. Technol.*, 2021, **55**, 9854–9863.
- 106 C. K. Remucal and M. Ginder-Vogel, *Environ. Sci.: Processes Impacts*, 2014, **16**, 1247–1266.
- 107 J. W. Stuckey, G. Christopher, W. Jian, L. A. Kaplan, V.-E. Prian, T. P. Beebe and D. L. Sparks, *Geochem. Trans.*, 2018, **19**, 6.
- 108 J. Chorover and M. K. Amistadi, *Geochim. Cosmochim. Acta*, 2001, **65**, 95–109.
- 109 Q. Wang, P. Yang and M. Zhu, *Environ. Sci. Technol.*, 2018, **52**, 1844–1853.



- 110 M. Rabe, D. Verdes and S. Seeger, *Adv. Colloid Interface Sci.*, 2010, **162**, 87–106.
- 111 W. Zhao, H. F. Cheng and S. Taos, *Environ. Sci. Technol.*, 2020, **54**, 1475–1483.
- 112 S. Allard, L. Gutierrez, C. Fontaine, J. P. Croué and H. Gallard, *Sci. Total Environ.*, 2017, **583**, 487–495.
- 113 K. Johnson, G. Purvis, E. Lopez-Capel, C. Peacock, N. Gray, T. Wagner, C. März, L. Bowen, J. Ojeda, N. Finlay, S. Robertson, F. Worrall and C. Greenwell, *Nat. Commun.*, 2015, **6**, 7628.
- 114 E. L. Trainer, M. Ginder-Vogel and C. K. Remucal, *Environ. Sci. Technol.*, 2021, **55**, 12084–12094.
- 115 E. Hu, S. Y. Pan, W. Z. Zhang, X. L. Zhao, B. Liao and F. He, *Environ. Sci.: Processes Impacts*, 2019, **21**, 2118–2127.
- 116 Q. Q. Li, X. C. Huang, G. J. Su, M. H. Zheng, C. H. Huang, M. J. Wang, C. Y. Ma and D. Wei, *Environ. Sci. Technol.*, 2018, **52**, 13351–13360.
- 117 Z. Q. Wang, H. Z. Jia, H. R. Zhao, R. Zhang, C. Zhang, K. C. Zhu, X. T. Guo, T. C. Wang and L. Y. Zhu, *Environ. Sci. Technol.*, 2022, **56**, 9806–9815.
- 118 Z. L. Chi, X. Y. Zhao, Y. L. Chen, J. L. Hao, G. H. Yu, B. A. Goodman and G. M. Gadd, *Environ. Microbiol.*, 2021, **23**, 893–907.
- 119 W. G. Sunda and D. J. Kieber, *Nature*, 1994, **367**, 62–64.
- 120 Y. C. Zhang, D. B. Yue, X. Wang and W. F. Song, *J. Environ. Sci.*, 2019, **77**, 167–173.
- 121 H. S. Qi, A. Zhang, Z. Du, J. Q. Wu, X. M. Chen, X. Zhang, Y. Zhao, Z. M. Wei, X. Y. Xie, Y. Li and M. Ye, *Waste Manage.*, 2021, **128**, 16–24.
- 122 W. C. Li, X. Y. Wen, X. J. Wang, J. Li, E. B. Ren, Z. F. Shi, C. M. Liu, D. Q. Mo and S. P. Mo, *Mol. Catal.*, 2021, **514**, 111847.
- 123 Z. Mengqiang, G.-V. Matthew, P. S. J, F. Xiong-Han and S. D. L, *Environ. Sci. Technol.*, 2010, **44**, 4465–4471.
- 124 R. M. Fang, Q. Y. Feng, H. B. Huang, J. Ji, M. He, Y. J. Zhan, B. Y. Liu and D. Y. C. Leung, *Catal. Today*, 2019, **327**, 154–160.
- 125 Y. Cheng, T. L. Huang, Y. K. Sun and X. X. Shi, *Chem. Eng. J.*, 2017, **322**, 82–89.
- 126 J. F. Zhong, J. M. Liu, R. Hu, D. D. Pan, S. C. Shao and X. W. Wu, *Bioresour. Technol.*, 2023, **377**, 128957.
- 127 Y. Song, Q. Pan, H. Z. Lv, D. Yang, Z. M. Qin, M. Y. Zhang, X. Q. Sun and X. X. Liu, *Angew. Chem., Int. Ed.*, 2021, **60**, 5718–5722.
- 128 J. C. Shu, Y. H. Wu, Y. L. Deng, T. Y. Lei, J. F. Huang, Y. H. Han, X. R. Zhang, Z. S. Zhao, Y. F. Wei and M. J. Chen, *Sep. Purif. Technol.*, 2021, **270**, 118798.
- 129 L. Zhang, J. L. Wang, H. X. Qiao, F. X. Liu and Z. S. Fu, *J. Cleaner Prod.*, 2020, **272**, 123055.
- 130 L. S. Balistrieri and T. T. Chao, *Geochim. Cosmochim. Acta*, 1990, **54**, 739–751.
- 131 T. Toshihiro, H. Kazuhito and N. Ryuhei, *J. Am. Chem. Soc.*, 2012, **134**, 18153–18156.
- 132 M. Zhu, C. L. Farrow, J. E. Post, K. J. T. Livi, S. J. L. Billinge, M. Ginder-Vogel and D. L. Sparks, *Geochim. Cosmochim. Acta*, 2012, **81**, 39–55.
- 133 A.-C. Gaillot, D. Flot, V. A. Drits, A. Manceau, B. Manfred and B. Lanson, *Chem. Mater.*, 2003, **15**, 4666–4678.
- 134 D. Banerjee and H. W. Nesbitt, *Geochim. Cosmochim. Acta*, 2001, **65**, 1703–1714.
- 135 H. Ouyang, C. Wu, X. H. Qiu, K. Tanaka, T. Ohnuki and Q. Q. Yu, *Environ. Res.*, 2023, **217**, 114874.
- 136 Z. G. Zhou, H. M. Du, Z. H. Dai, Y. Mu, L. L. Tong, Q. J. Xing, S. S. Liu, Z. M. Ao and J. P. Zou, *Chem. Eng. J.*, 2019, **374**, 170–180.
- 137 J. Z. Huang, Y. F. Dai, K. Singewald, C. C. Liu, S. Saxena and H. C. Zhang, *Chem. Eng. J.*, 2019, **370**, 906–915.
- 138 L. Hui, S. Fernanda, B. Kristen and H. Elizabeth, *Environ. Sci. Technol.*, 2021, **55**, 12136–12152.
- 139 P. Márta, G. Ildikó, F. Krisztián, H. Henrietta, P.-M. Elemér and B. J. Carlos, *Front. Microbiol.*, 2019, **10**, 2731.
- 140 D. R. Learman, B. M. Voelker, A. I. Vazquez-Rodriguez and C. M. Hansel, *Nat. Geosci.*, 2011, **4**, 95–98.
- 141 T. Yuanzhi, Z. C. A, S. C. M and H. C. M, *Environ. Microbiol.*, 2013, **15**, 1063–1077.
- 142 D. L. Chaput, A. J. Fowle, S. Onyou, D. Kelly, C. M. Hanse and C. M. Santelli, *Sci. Rep.*, 2019, **9**, 18244.
- 143 M. Polgári and I. Gyollai, *Ore Geol. Rev.*, 2021, **136**, 104203.
- 144 C. M. Hanse, *Adv. Microb. Physiol.*, 2017, **70**, 37–83.

